Mineralogical and geochemical characteristics of the Amensif Cu, Pb, Zn, (Ag, Au) ore deposit, Western High Atlas, Morocco

Saïd Ilmen[1*], Abdelkhalek Alansari[1], Amine Bajddi[2], Aomar Ennaciri[2], Lhou Maacha[2]

1- Department of Geology. Faculty of Sciences-Semlalia, Cadi Ayyad University, Marrakesh, Morocco
2- Managem mining Company (SA), Twin Center, Casablanca, Morocco

* Corresponding Author: said.ilmen@edu.uca.ma

Abstract

The Cu, Pb, Zn, Ag-Au deposit of Amensif is located on the northern flank of the western High Atlas. This deposit is hosted in Lower Cambrian carbonate bars and is structurally controlled by NE-SW to E-W trending fault structures and is spatially associated with the Permian 273 Ma Azegour granite. Ore reserves are around 0.5 Mt and grades are 3.21% Zn, 0.58% Pb, 0.86% Cu with 83.31 ppm Ag and 0.41 ppm Au. Sulphide mineralizations occur as a local replacement of carbonate bars rocks. Ore mineralization at Amensif is dominantly composed of chalcopyrite, sphalerite, galena, pyrite and arsenopyrite. Gold is hosted by arsenopyrite and silver was associated with galena and tetrahedrite-tennantite. Gangue minerals include predominantly chlorite, epidote, tremolite, calcite, dolomite, quartz, sericite, minor andradite and vesuvianite. We have recognized three major hydrothermal transformations that affected carbonate bars: intense silicification, hydrothermal dolomitization, locally skarnification and retrograde alteration. Silicification is the main hydrothermal alteration that was accompanied by important replacement textures between sulphide minerals. Lead isotope compositions of galena sampled from two regions in western High Atlas (Amensif and Tighardine) show a short range in $^{206}Pb/^{204}Pb$ (18.053–18.324), $^{207}Pb/^{204}Pb$ (15.534–15.577) and $^{208}Pb/^{204}Pb$ (37.780–37.986) and extend from relatively unradiogenic sulphides to radiogenic and internally inhomogeneous isotopic composition. The Pb isotope signature suggests that Pb-Cu-Zn minerals were generated during the remobilization of lead from the older reservoir in the Cambro-Ordovician volcano-sedimentary units. Combined field, lithological, structural, mineralogical and geochemical data of the Cambrian carbonate-hosted mineralization at Amensif deposit is compatible with polymetallic carbonate replacement deposit type mineralization.

Keywords: Carbonate Replacement Deposit, Replacement Textures, Chalcopyrite Disease, Lead Isotopes, Cambrian, Amensif, Western High Atlas, Morocco.

1– Introduction

The geology of the Amizmiz area is known through the exploration and mining activities related to the historical discovery in 1919 of the W-Mo-Cu Azegour mine, Zn-Pb-Cu-Ag Assif El Mal mine in 1920 and Zn-Pb-Ag Erdouz mine in 1927 (Permingeat, 1957).

The Amensif deposit was discovered in the 2006, by the prospectors of the Amensif Manajim Company. After, the deposit was acquired by the Guemassa Mining Company who developed an active mine in the area. Our studies on the region were started since 2006 (Alansari *et al.*, 2009; Ilmen, 2011). Through field studies, we identified many other deposits in the region such as the Amensif, Talat n' Imjjad and Ibardaten deposits.

The present study is focuses on the Amensif polymetallic Cu-Zn-Pb (Ag-Au) deposit. This latter is located 85 Km southwest of Marrakesh city on the northern flank of the western High

Atlas. Initial estimates of reserves at the base of 18% dilution and recovery of 85%, are in the order of 569 814 Tons with; 3.21% Zn, 0.58% Pb, 0.86% Cu with 83. 31 ppm Ag and 0.41 ppm Au.

The aim of this paper was to clarify and elucidate the formation conditions of this mining area in terms of nature and ore genesis, petrographic, mineralogical and geochemical data and described the evolution of hydrothermal alteration, in order to deduce the typology and style of the polymetallic mineralizations.

2– Background geology

Geotectonically, the Amensif deposit is located in the western High Atlas. It is located about 85 km in the SW of Marrakesh and about 5 km in the south of the famous Azegour W-Mo-Cu mine (Permingeat, 1957). The deposit lies at the intersection of NE and NW trending tectonic belts between the Erdouz fault zone and the Al Medinat fault zone. The ore deposit is hosted in the Lower volcano-sedimentary terranes, overthrust by Cretaceous sedimentary terranes. The Lower Paleozoic formations are belonging to the Lower and Middle Cambrian and were intruded by tardi-Hercynian granite of Azegour (271 ± 3 Ma; Mrini *et al*., 1992) and by intermediate to felsic dikes (Fig. 1).

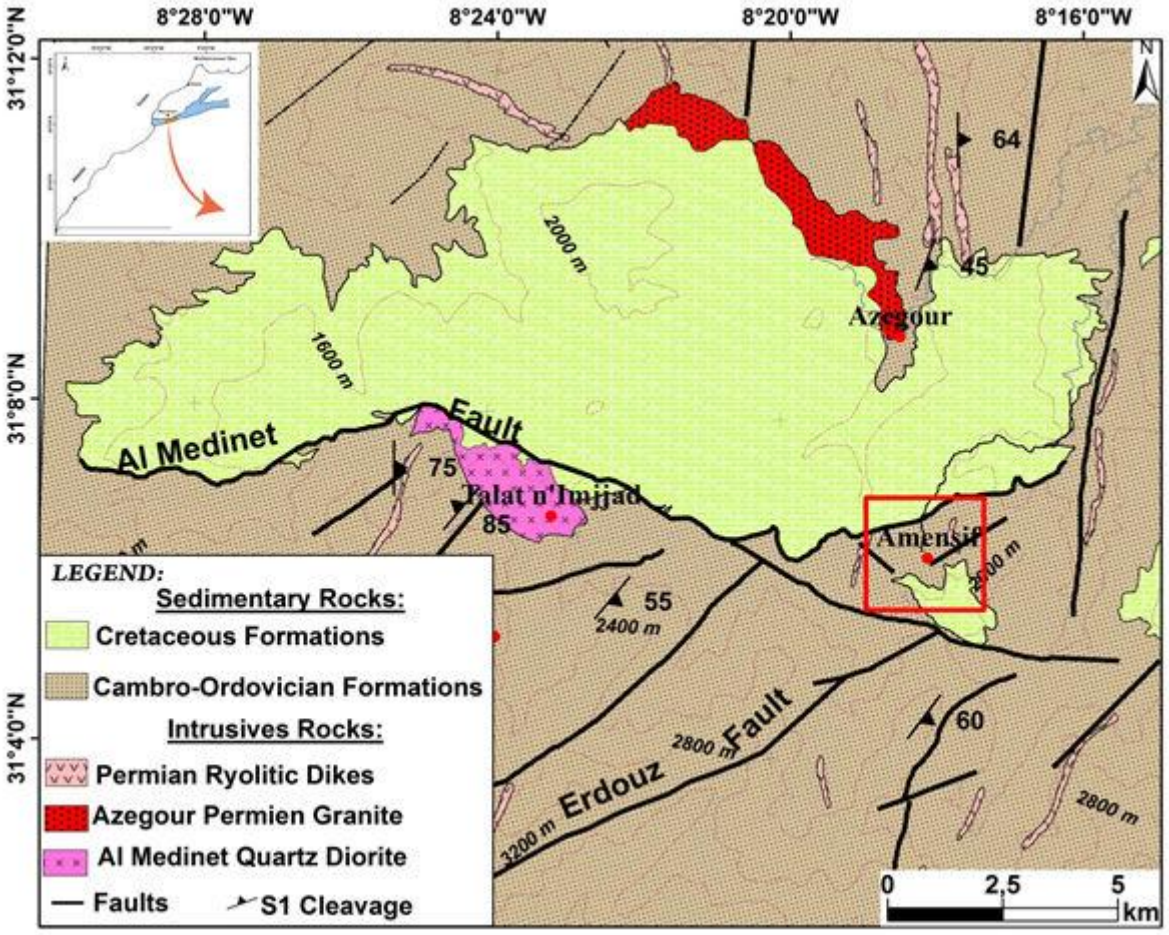

Figure 1) Simplified regional geological map of the Guedmiwa Region showing the major tectonic structures and the emplacement of the plutonic ores and location of the study area (Modified from Labriki, 1996; Dias et al., 2011).

2.1– Stratigraphy

The stratigraphy of the studied area consists of a thick succession (about 600 m) (Cornée *et al*., 1987a, 1987b; El Archi, 1989; Badra, 1993; Labriki, 1996; Bouabdellah *et al*., 2009) of a Cambrian metasedimentary and volcaniclastic sequence overthrust by Cretaceous sedimentary terranes (Fig. 2). The metasedimentary sequence was regionally affected by a low-grade

metamorphism (green schists) (Cornée *et al.*, 1987a).

Two stratigraphic units can be distinguished: a lower volcano-sedimentary units and an upper pelitic unit.

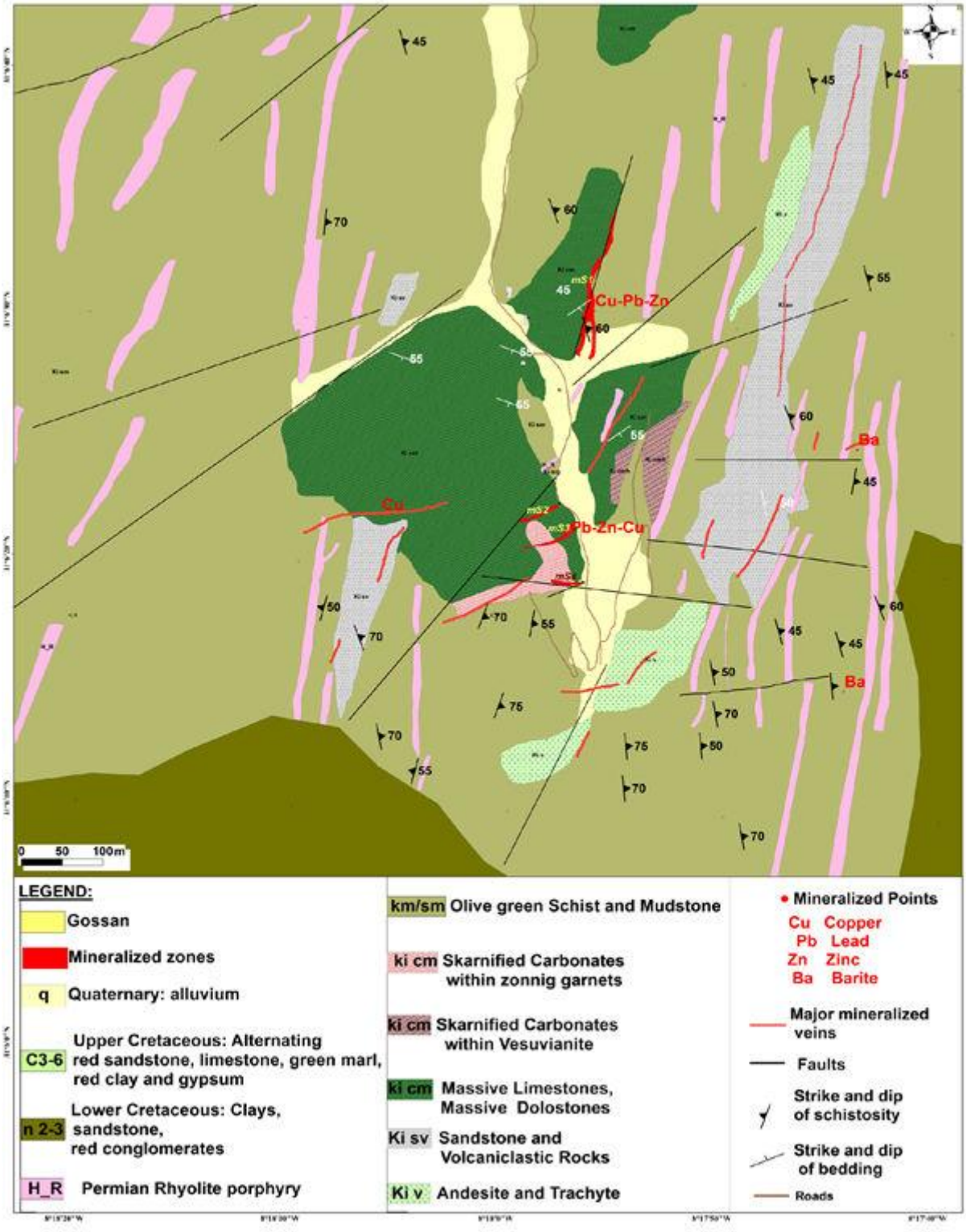

Figure 2) Detailed geological map of the Amensif Deposit showing the relationship between mineralization carbonate hosted-rock and the major faults.

The simplified stratigraphic sequence in the mine area is sketched in figure 3 from the base to the top we distinguish:

- A lower unit composed of carbonate rocks (limestones, marbles and dolostones) overlain by calcareous and pelitic schists and calc-schists (Fig. 4A). This lower unit was

marked by alternating limestone bars and lenses interlayered with calcareous schists, volcano-clastic, metalavas and pyroclastic rocks (Fig. 4B). This unit is clearly related to the Lower Cambrian by analogy with the same unit in the Anti-Atlas (Neltner, 1938; Badra, 1993; Ouazzani *et al.*, 2001; El Archi *et al.*, 2004; Alansari *et al.*, 2009; Ilmen, 2011).

- An upper unit composed predominantly of sandstones and green schists. Also, by analogy, we attribute this unit to the Middle Cambrian (Fig. 3) (Ilmen, 2011).

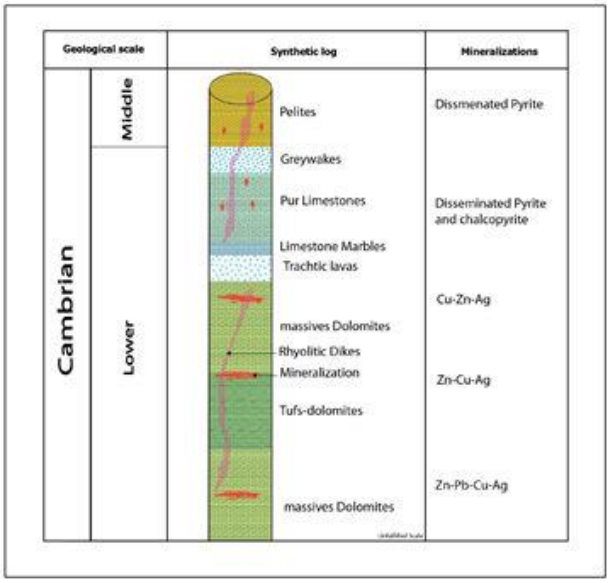

Figure 3) Stratigraphic column of the Amensif deposit.

Figure 4) Field drill core photos of the Amensif deposit (A) photo showing the dolomite bar (B) photo of mylonitized trachyte. (C) Drill core photo showing the silicified and brecciated limestones. (D) Skarnified Carbonates. (E) Silicified zone on the carbonate bars. (F) Photo showing the gossan zone with malachite and azurite. (G) Massive sphalerite in drill core. (H) Disseminated chalcopyrite in drill core.

2.2– Magmatic activity

Magmatic activity in the region is marked by two major events; (i) as first major event; the region is characterized by an intense volcanic activity during the Lower Cambrian (Cornée *et al.*, 1987a; Badra, 1993) (Fig. 1). The products of this activity are represented mainly by lavas flows. These lavas are attributed to basaltic, andesitic calc-alkaline series (Ouazzani *et al.*, 2001; Pouclet *et al.*, 2008; Ilmen, 2011). According to Pouclet *et al.* (2008), this volcanic activity is dated at 533 ± 4 Ma by $^{206}Pb/^{238}U$ and $^{207}Pb/^{206}Pb$ methods. In 2011, we have revealed the presence of trachyte for the first time in western High Atlas (Ilmen, 2011) (Figs. 4B, 5F).

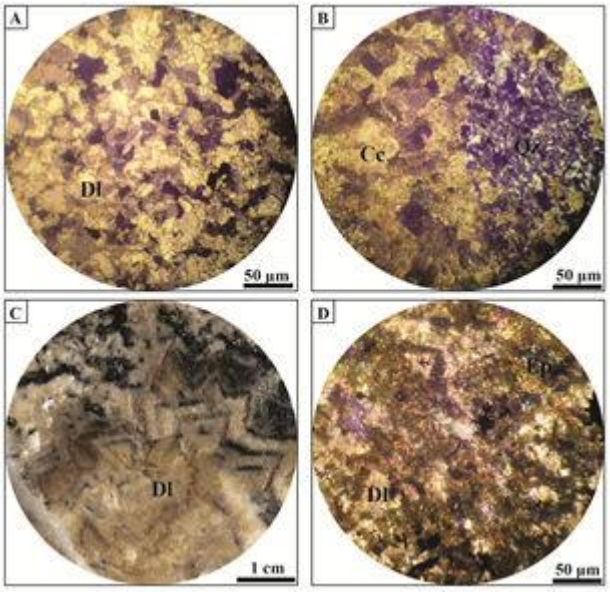

Figure 5) (A) Photomicrographs showing the dolomite minerals. (B) Photomicrograph showing silicified. (C) Photograph of saddle dolomite crystals showing concentric growth zones (wedge development). (D) Photomicrograph showing replacement between epidote and dolomite (hydrothermal dolomite).

(ii) As second major event during the Permian, the Cambrian volcaniclastic and metasedimentary sequence is intruded by a suite of 347 to 273 Ma high-level synorogenic to postorogenic Hercynian granitoids (Permingeat, 1957; El Amrani, 1984; Mabkhout *et al.*, 1988; Amenzou and Badra, 1996; Bouabdellah *et al.*, 2003, 2009) Azegour granite and Al Medinet quartz diorite and by intermediate to felsic dikes that postdate regional deformation and associated metamorphism, show several phase of deformation and is mostly metamorphosed to green schist facies (Bouabdellah *et al.*, 2009). Numerous microgranitic to porphyry rhyolitic dikes cross-cut the Amensif section and trend NNW-SSE to N-S. This swarm of dikes is perhaps genetically attributed to the post-Hercynian granite of Azegour. This granite gives age of 273 ± 3 by Rb/Sr (Mrini *et al.*, 1992).

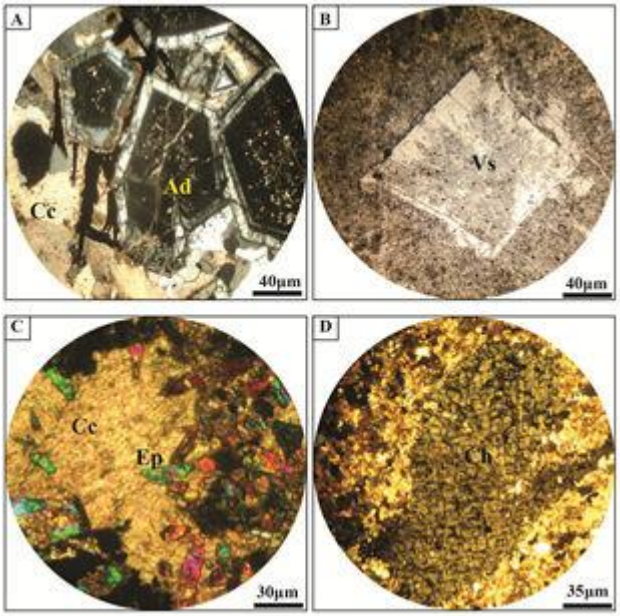

Figure 6) (A) Photomicrograph of subhedral andradite crystal showing concentric-oscillating zoning. (B) Photomicrograph of prismatic phenocrystal of vesuvianite. (C and D) Photomicrographs showing replacement between calcite/ dolomite and epidote and or chlorite Mineral abbreviations: Dl-dolomite; Cc-calcite; Ep-epidote; Ad-andradite; Vs- vesuvianite.

2.3– Structural setting

The units described above are exposed within a tectonostratigraphic domain limited by two major shear zones: the Al Medinet fault in the north and the Erdouz fault in the south (Fig. 1). These major faults are participated to make a history of the Hercynian orogeny of western High Atlas. Locally, the Paleozoic series of Amensif records three Hercynian phases of deformation (Ait Ayyad, 1987; Prost *et al.*,

1989; Ouanaimi and Petit, 1992; Labriki, 1996; Dias *et al*., 2011). The first event (D1) led to the formation of flow schistosity S1 subparallel to the stratification S0, associated with interfolial micro-folds and stretching lineation L1 (Bouabdellah, 1988; Pouclet *et al*., 2008; Bouabdellah *et al*., 2009). The framework found is very homogeneous. The D1 structures have a remarkably constant north-south trend well defined by related folding and cleavage. This cleavage is axial planar to tight major folds frequently transposing the bedding planes. In some place, the north-south trending structures are deflected to NE-SW trending by the development of the D1 shear zones. The second phase (D2) develops N-S trending tight folds commonly associated with S2 fracture cleavage or flow schistosity sometimes parallel to S0-1. The third ductile deformation (D3) generates N70 trending isoclinal folds, associated with cleavage S3, varying from fracture to flow schistosity. Faults and fissures within the Amensif section, trend N-S to NNE-SSW and ENE-WSW to E-W (Fig. 1).

3– Analytic methods

Field work included geological mapping, delineating approximately the carbonated bars carrying the mineralization and surveys of core drilling and sampling. All samples were collected from the surface and cores in mineralized intercepts. 20 polished and 25 thin sections were prepared and examined microscopically for petrographic study. Four representative samples were studied by XRF spectrometer using a MagiX of PANalytical instrument with Rh radiation at the Reminex's Research Center and Laboratory of Marrakesh for determining the composition of calc-silicates such as garnets and vesuvianite.

Metal element analyses were carried out at the Reminex's Research Center and Laboratory of Marrakesh with an ICP-AES (Jobin Yvon ULTIMA 2c) with mono- and polichromators. 33 samples were analysed for Fe, As, Cu, Pb, Zn, Ag and Au elements.

Lead isotope analyse was carried out on galena mineral separates which were hand -picked from two samples collected from the ores in Amensif Area. Two samples were analysed for Lead isotopic composition at the GEOTOP Laboratory-UQAM, Canada.

4– Structure of the deposit

Extensive mapping of the mineralized zones since 2011 has revealed several important geological and structural attributes highlighting their mode of emplacement and formation. The mineralization consists of polymetallic Cu-Zn-Pb-Ag-Au veins injected in Lower Cambrian limestones and located in close proximity to a swarm of rhyolitic dikes. The ore veins are oriented parallel to the Erdouz ENE-WSW trending fault. Replacement ore bodies are the most interesting ones from genetic and economic aspect and variable from morphological point of view. They are always embedded in the carbonate horizons of the deposit (Fig. 2). Their thickness is generally 30-50 cm, sometimes even more.

The host carbonate rocks are commonly silicified, locally replaced by calci-silicate skarn minerals near their contact with igneous rocks and finally dolomitized (Figs. 3, 4C-D, 5 and 6). Ore textures in the replacement ore bodies are rhythmic-banded, impregnations, massive, or replacement texture (Figs. 7 and 8A-F). The sulphide orebodies are extremely irregular shape, lenticular and veined. The massive, coarse-grained metasomatic sulphide ores are characterized by high porosity. A system of open space cavities are often developed within the skarn bodies as a result of selective dissolution mainly of the retrograde carbonates.

Four main mineralized structures (mS) are distinguished (Fig. 2) based on mineral assemblages, associated hydrothermal alterations and their geometries. The northern

structure (mS1) striking NNE-SSW is relatively long (max 200 m), 2 m large and it is marqued by Cu-Pb-Zn-Ag-Au minerals. The mS1 orebody is characterized by chalcopyrite (abundant) pyrite, arsenopyrite, galena, sphalerite and tennantite-tetraedrite. The gangue minerals are marqued by abundance of quartz + calcite+ chlorite+ dolomite and minor epidote+ tremolite. Orebodies mS2, mS3 and mS4 are oriented respectively N60°, N70° and N110° and are economically most important (Fig. 2). Ores from these orebodies are very rich on Zn-Pb-Cu-Fe-As-Ag-Au minerals. The mineral assemblages of these structures are sphalerite, galena, chalcopyrite, pyrite and arsenopyrite. The gangue minerals are calcite, dolomite, chlorite, epidote, tremolite, quartz and minor of andradite + vesuvianite. An important gossan marqued the mS4 orebody.

Ore structures are dominated by massive accumulations of sulphide minerals, but may be veined, disseminated and brecciated.

4.1– Hydrothermal alteration

Styles of wall-rock alteration in the Amensif deposit are relatively simple and present similar characteristics of the Carbonate replacement deposits around the world (e.g. Eureka district in Nevada, USA; Cox, 1986; Morris, 1986; Vikre, 1998).

At Amensif deposit, three main hydrothermal transformations are recognized. Silicification and hydrothermal dolomitization are the abundant hydrothermal alterations in the area. These alterations are responsible for the recrystallization of the limestone wallrocks to variant degree (silicified limestones, marble). The microcrystalline calcite and dolomite of the limestones has been almost completely replaced by quartz as a result of an intense silicification (Figs. 5A and B). The hydrothermal dolomitization is last one developed and it is marqued by recrystallization of limestones and development of saddle dolomite. The skarnification is relatively weak and it is limited to an area of 20 m^2 in surface. It is present only in the immediate contact with rhyolitic dikes. This skarnification is marqued by development of anhydrous and hydrous skarn minerals. Anhydrous minerals are andradite and vesuvianite charactering the prograde alteration. Intense retrograde alteration is common in skarns (Einaudi, 1982; Meinert, 1992; Calagari and Hosseinzadeh; 2006; Canet *et al*., 2009; 2011) and in some carbonate replacement deposits may destroy most of the prograde anhydrous calc-silicates (Cox, 1986; Morris, 1986). At Amensif, retrograde alteration is characterized by hydrous mineral assemblages composed of epidote + chlorite + tremolite + quartz + calcite + sericite minerals (Figs. 4C-D-E, 5A-F and 6).

The main hydrothermal minerals identified are:

Quartz occurs as fine-to medium grained (up to 0.8 mm across) patchy aggregates, dispersed and solitary crystals and as veins and veinlets within the calc-silicates. Strong silicification replaced most former minerals by quartz (Fig. 5B).

Small amounts of ***sericite*** are observed with chlorite and quartz.

Dolomite occurs as fine grained to coarse anhedral to subhedral mainly 20–200 μm in size within the hydrothermal zones. Hydrothermalized dolomite displays color varying from dark gray to green (Figs. 5A-D). The micro- and pseudospar textures of the Amensif dolostone are replaced by closely packed anhedral saddle dolomite with undulatory extinction (Fig. 5D). Medium to coarse grained crystals (1 to 7 mm) are also present in veinlets cutting other mineral aggregates, where they show different texture and are accompanied by very fine to coarse crystals (1 to 10 mm) of dolomite and ankerite and sericite (Figs. 4G, H and 5A, B). Some carbonate minerals are partially and locally replaced by calc-silicate minerals (Figs. 6 A, B and C). In comparison with non-altered

dolomite, this later occurs in coarse-crystalline euhedral rhombs, granular, massive and irregular forms. The intensity of dolomitization increases with increased depth.

Chlorite is very abundant, both in mineralization, the footwall altered pelites and the carbonates. In the calc-silicates rich units, it occurs as up to 350 µm-wide platelets that can form Spherulitic aggregates, commonly in association with quartz, epidote, calcite and tremolite (Fig. 6D).

Epidote is a second component abundant of the mineralization after chlorite, as it occurs in all the calc-silicate assemblages, in the sulphide mantos and in the footwall altered metasedimentary rocks. Its main occurrence is as microcrystalline epidote-chlorite assemblages with quartz, calcite, andradite, tremolite and sulphides (chalcopyrite, galena, sphalerite and pyrite). Epidote occurs as euhedral prismatic crystals (Figs. 5D and 6C).

Tremolite occurs as Spherulitic crystals commonly associated with chlorite, epidote and calcite. It is abundant in the footwall altered metapelites. Tremolite is partially replaced by chlorite.

Andradite: Field and petrographic observations show a locally presence of garnet-mineral hosted by marble and metamorphic limestones cross-cutted by the rhyolitic dikes. Under microscope, andradite appears commonly as fine-grained subhedral forms (Fig. 6A). Crystals are as large as 5 to 7 mm in diameter. Petrographic characteristics and XRF analysis of garnet sample correspond to the characteristic of andradite (calcic-garnet) mineral. Most of the andradite crystals had coarse concentric-oscillating zoning and sector twins distinguished by color and chemical composition (Ivanova *et al*., 1998). Andradite is associated with quartz, calcite, chlorite, epidote, pyrite, galena and chalcopyrite.

Vesuvianite occurs mostly in metamorphic limestones as euhedral, randomly oriented prismatic phenocrysts a few tens of µm to 6 mm (Fig. 6B). The vesuvianite sample is analyzed and studied by XRF. Data analysis confirmed the presence of association of F-rich vesuvianite, quartz and calcite.

4.2– Sulphide Mineralization

The paragenetic sequence observed in the studied samples is summarized in Figure 7. Two stages of mineralization are defined based on relationships and textures between minerals.

With incident light, a variety of sulphide minerals was recognized in the ores at the Amensif deposit. The main veins and secondary veins have different internal textures. Replacement textures suggest that the mineralization formed for the most part at the expense of the carbonate beds of the Lower Cambrian sequence, in an epigenetic, hydrothermal metasomatic stage.

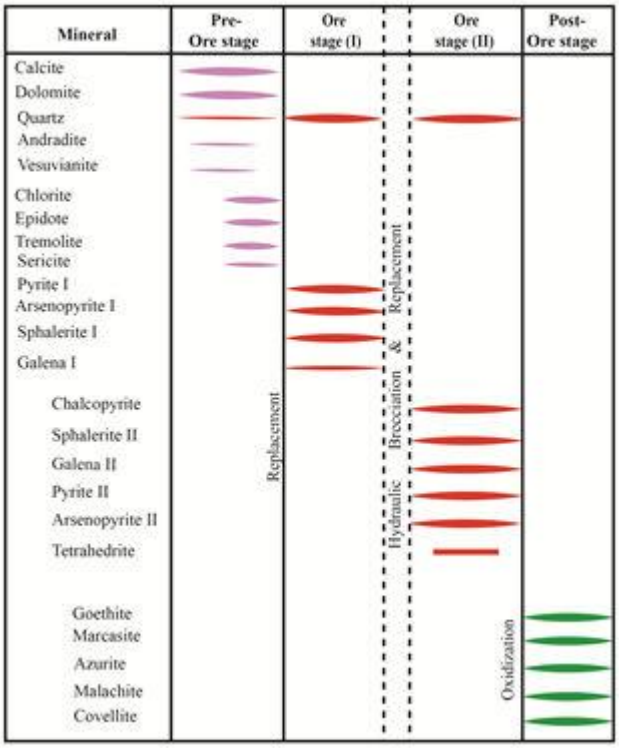

Figure 7) Simplified paragenetic sequence of the assemblages of main ore in the Amensif deposit.

Ore stage (I):

This stage refers to deposition of early pyrite, arsenopyrite and early sphalerite (I) with minor of galena (I). These minerals are accompanied with crystallization of quartz and calcite. Pyrite

(I) and arsenopyrite (I) are cogenetic with the slightly delay between the beginning of crystallization of pyrite, and occur as coarse-grained (2–5 mm). Early Sphalerite (I) and galena are post-crystallization of pyrite and arsenopyrite assemblage. This stage is characterized by intensive hydraulic brecciation of pyrite-quartz assemblage. The fractures were cemented by paragenetic sulphide of the second stage.

Ore stage (II):

Ore stage (II) is the main focus of the mining activity in the Amensif deposit. The sulphides present, in decreasing order of abundance, are chalcopyrite, sphalerite, galena, pyrite, arsenopyrite and tetrahedrite-tennantite. This stage is mainly characterized by strong replacement texture between sulphide minerals. An important replacement of the early sphalerite and galena by chalcopyrite, tetrahedrite-tennantite, late pyrite (II) and late arsenopyrite (II) is observed (Figs. 9A and B). Late sphalerite (II) appears with blebs of chalcopyrite or entirely replaced by chalcopyrite and galena (II). Pyrite and arsenopyrite are partially or entirely replaced by chalcopyrite. In contrast with the first stage, late pyrite (II) and arsenopyrite (II) occur in fine-grained size aggregates. This reduction in size due to thermo-barometric conditions changed. Formation of fine arsenopyrite grains probably enriched in gold seems to occur under considerable oversaturation of hydrothermal solutions with S-As-containing complex compounds of gold, whose decomposition results in a great number of sulphide seeds, which rapidly crystallize (Volkov *et al*., 2006). The frequently occurring paragenesis of arsenopyrite with pyrite-containing sedimentary rocks and the widespread growth of high-Au arsenopyrite over globular-crystalline pyrite aggregates are the evidence of the crucial role of syngenetic pyrite in the deposition of gold-containing arsenopyrite (Kovalev *et al*., 2011).

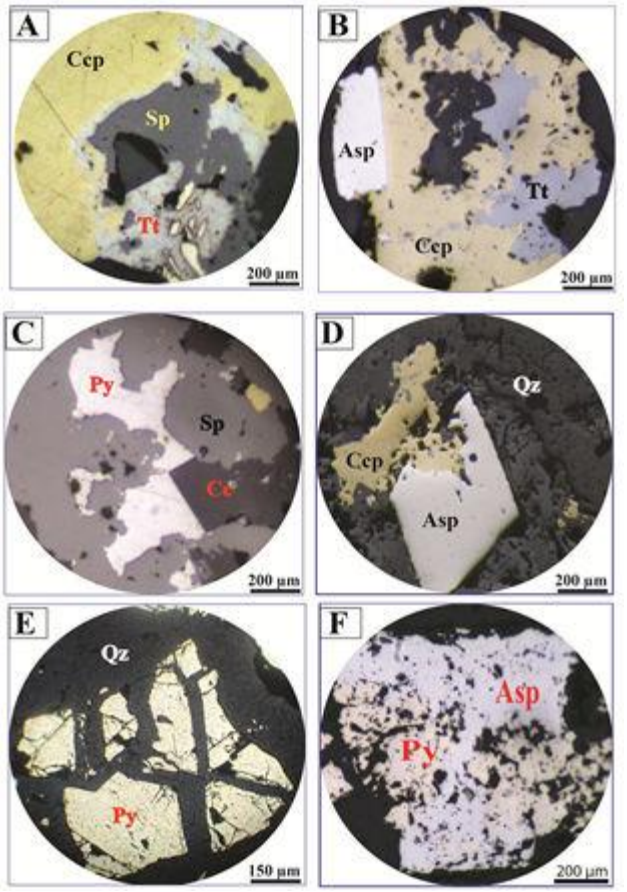

Figure 8) Photomicrographs in reflect light of textural relationships among ore minerals. (A) Chalcopyrite, sphalerite and Tetrahedrite-tennantite. Note that, tetrahedrite-tennantite replaces sphalerite and arsenopyrite (totally replaced). (B) Typical occurrence of tetrahedrite-tennantite included in chalcopyrite associated with euhedral rhombic crystal of arsenopyrite. Note that, the initial replacement of arsenopyrite by chalcopyrite. (C) Replacement texture showing late sphalerite replacing early pyrite. (D) Replacement texture showing initially replacement of arsenopyrite by chalcopyrite. (E) Photomicrograph showing early pyrite brecciated. (F) Photomicrograph showing cogenetic crystallization between early pyrite and arsenopyrite. ***Mineral abbreviations****: Ccp-chalcopyrite, Py-Pyrite, Sp-Sphalerite, Gn-Galena, Asp-Arsenopyrite, Tt Tetrahedrite-tennantite, Qz-Quartz, calcite Cc.*

This stage is identified based on the replacement between sulphide minerals. Gold is hosted mainly by arsenopyrite and silver is closely associated with tetrahedrite-tennantite.

Supergene stage:

This stage includes oxidation and supergene enrichment of the ore. During this stage, majority of primary minerals are oxidized by secondary paragenetic minerals. Pyrite was replaced by goethite and marcasite. Covellite replaces chalcopyrite, sphalerite and tetrahedrite-tennantite. Chalcopyrite was also replaced by covellite, malachite and azurite (Fig. 4F).

4.3– Ore Mineralogy

Detailed field and microscopic examinations indicated that the dominant ore minerals in the Amensif deposit are chalcopyrite, sphalerite, galena, pyrite and arsenopyrite, with a minor tetrahedrite-tennantite. The supergene stage is characterized by the transformation of chalcopyrite to malachite and or azurite, pyrite to goethite (Figs. 8A and F).

In the following paragraph, the main minerals in the Amensif deposit will be described.

Chalcopyrite:

Chalcopyrite is a major phase in the main Cu-Pb-Zn-Ag-Au orebody (mS1). It is fine- to high-grained (>1 mm) and occurs as interstitial disseminations or as patchy aggregates with mutual interference boundaries against the main sulphides. Chalcopyrite is usually homogeneous (Figs. 8A, B and D), but in some places contains very fine-grained of sphalerite that replaced (Figs.9A andB). Chalcopyrite is observed also as some blebs in sphalerite. These blebs of chalcopyrite are called chalcopyrite disease (Fig. 9C) (Barton and Bethke, 1987). Microscopic examinations indicate the presence of tetrahedrite-tennantite closely associated with chalcopyrite.

Sphalerite:

Sphalerite occurs as massive, porphyritic, banded and disseminated aggregates commonly with chalcopyrite, galena, pyrite, arsenopyrite, quartz, calcite and other minerals in Zn-Pb-Cu-Fe-As-Ag-Au orebodies (mS2, mS3 and mS4). It is fine- to moderately coarse-grained (0.5 to 10 mm) and has a xenomorphic–subidiomorphic granular texture. They are diverse in color, commonly brown and brownish-yellow. Sphalerite is a ubiquitous sulphide in all the orebodies at Amensif and it is the most abundant ore mineral on a deposit scale. Sphalerite is also disseminated in the host-rock massive dolomite and in the carbonaceous dolomite. In the second ore stage, sphalerite occurs as anhedral crystals filling cracks and fractures affected old pyrite formed during the first stage (Fig. 8C). It contains a small oriented blebs and inclusions of chalcopyrite (chalcopyrite diseases). These blebs intergrowths indicate high temperature cogenetic formation of chalcopyrite and sphalerite from a parent Cu–Zn–S solid solution (Barton and Bethke, 1987; Ramdohr, 1969).

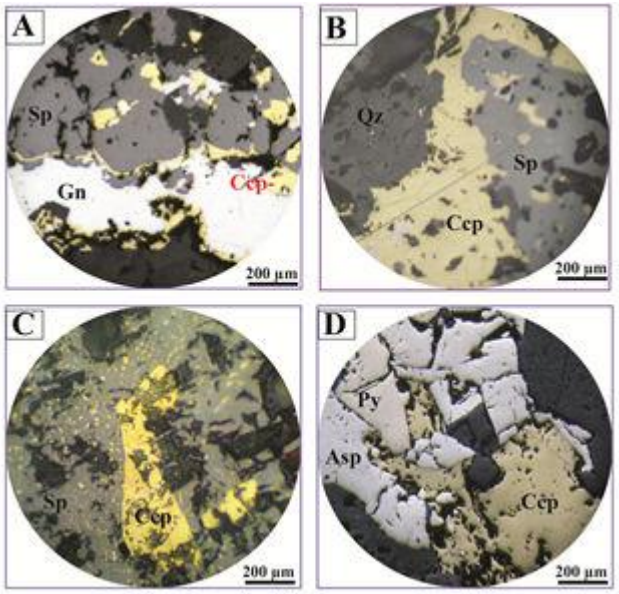

Figure 9A) Nice banding of chalcopyrite, galena and sphalerite resulting from replacement texture. (B) Replacement texture showing chalcopyrite replacing sphalerite. (C) Photomicrograph showing blebs of chalcopyrite in sphalerite. (D) Association of pyrite, arsenopyrite, chalcopyrite and quartz. Note that, chalcopyrite filling fractures of pyrite and arsenopyrite.

Galena:

Galena occurs as moderately coarse-grained (0.5 to 15 mm), euhedral grains that usually occur as aggregates in coexistence with sphalerite, pyrite and calcite and cubic crystals

are present. It is closely associated with sphalerite, chalcopyrite and pyrite (Fig. 9A). Geochemical Analyses indicate that galena was enriched by silver.

Pyrite:

Pyrite is a major ore sulphide characterizing the first ore stage. It occurs as aggregates and monominerallic cubic crysts up to 0.6mm across.

Two generations of pyrite were distinguished at Amensif. The first one is formed during the early stage (I). It is typically euhedral coarse-grained (1-3 mm). Pyrite shows also brecciated texture in fractures zones. It is entirely fractured and replaced by chalcopyrite and sphalerite formed during the last stage (II) (Figs. 8E, 9D). During the first stage, pyrite is associated with arsenopyrite and quartz (Fig. 8F). The second generation of pyrite is attributed to the last stage. It occurs as fine-grained and forms aggregates and intergrowths as micro-euhedral cubes within arsenopyrite. The textural relationships between pyrite and arsenopyrite indicate a cogenetic crystallization with slightly delay between the beginning of the formation of pyrite. This latter was affected by a supergene alteration and it is successively pseudomorphosed to goethite.

Arsenopyrite:

At the first carbonate ore stage sulphides continued to precipitate characteristically as arsenopyrite and pyrite. Arsenopyrite occurs as euhedral rhombic crystals and formed aggregates within pyrite (Figs. 8B and D). Arsenopyrite occurs as two generations at Amensif. The first one is characterized by the monominerallic aggregates, the grains are idiomorphic with a coarse-grained size (0.4 to 5 mm). It is associated with coarse-grained pyrite formed during the first Fe-As ore-stage. During this stage, pyrite and arsenopyrite are affected by an intensively hydrothermal brecciation. Replacements are so frequent for arsenopyrite. The second generation of arsenopyrite is characterized by fine grained associated with fine grained size of pyrite formed during the last stage (II) (Fig. 8F).

Tetrahedrite-tennantite is moderately represented in Amensif deposit. It was observed either as inclusions or as coarse grains in chalcopyrite. It also observed as large bands associated with sphalerite or with galena (Figs. 8A and B).

4.4– Geochemistry

Copper and zinc are the most abundant metal at the Amensif deposit. The potential for Cu-Pb-Zn ores in the deposit initial has been tested by drill programs. The initial estimates for reserves are in the order of 569 814 Tons with; 3.21% Zn, 0.58% Pb, 0.86% Cu with 83.31 ppm Ag and 0.41 ppm Au.

Figure 10 shows the correlations between Ag versus As; Au versus As, As versus Fe, Au versus Ag, Cu versus Pb, Zn versus Pb. The Correlation between Ag, Au, As, Fe, Zn and Pb shows a moderate positive correlation with weak square of the correlation coefficient (R2) which varying from 0.0199 to 0.4796. Except, the Cu versus Pb diagram that shows a stable correlation. These correlations reflect the close mineralogical association between Au, Ag, As, Fe, Pb and Zn minerals. Cu, Zn, Pb, Ag and Ag are systematically presented in significant amounts. This deposit is characterized by a particular high ore grade (Table 1) and by a simple ore mineral assemblage (chalcopyrite, sphalerite, galena, pyrite, arsenopyrite, tetrahedrite-tennantite, calcite and quartz). The chemical data of Amensif deposit is given in Table 1.

The use of lead isotope in ore genesis is especially helpful to define the source material of the ore lead. On the basis of the result of two lead isotopic data ($^{206}Pb/^{204}Pb$ (18.053–18.324), $^{207}Pb/^{204}Pb$ (15.534–15.577) and $^{208}Pb/^{204}Pb$ (37.780–37.986)); the metallogenic event that gave rise to the polymetallic mineralization of

Amensif is attributed to the Cambro-Ordovician event.

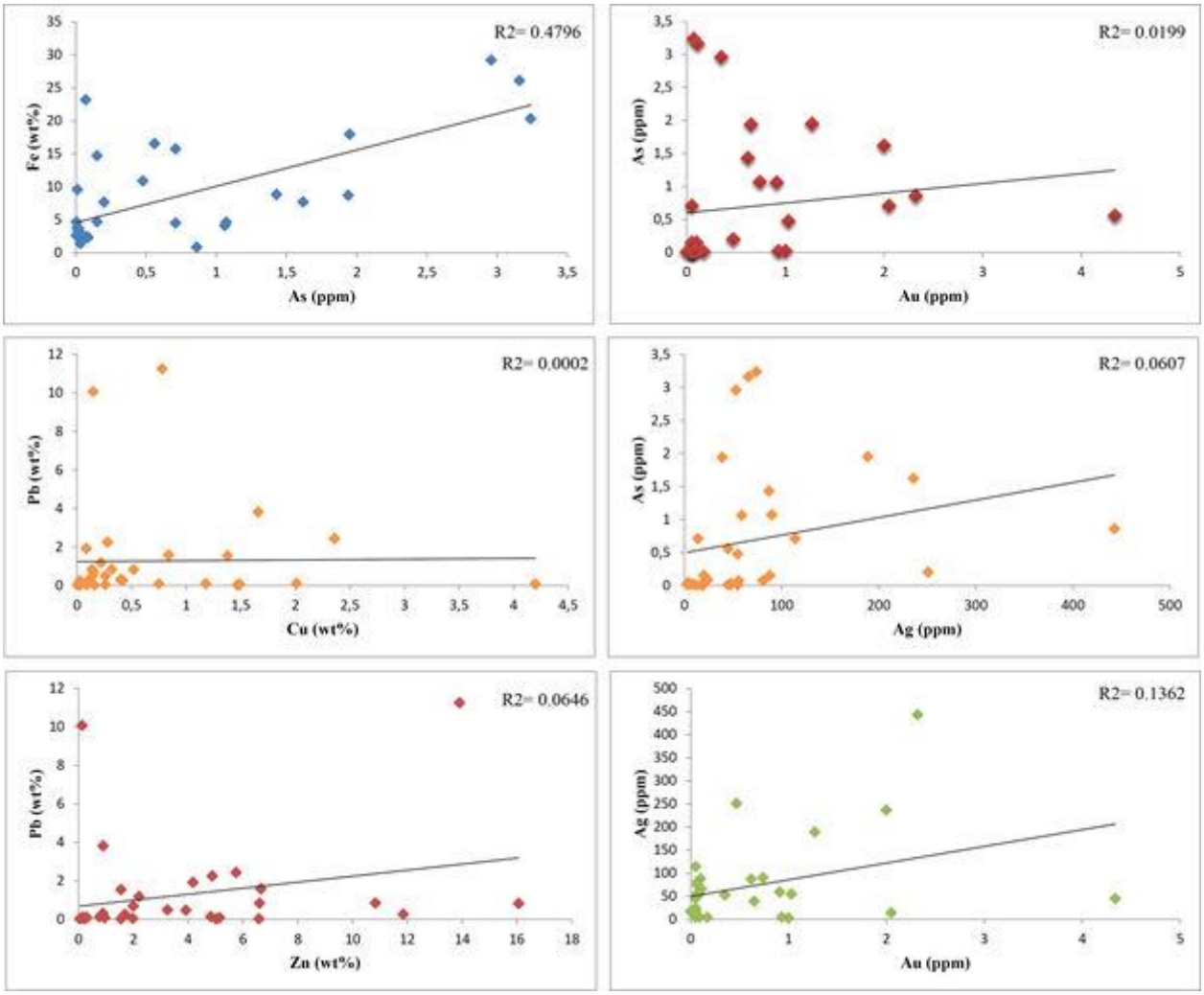

Figure 10) Correlation diagrams of Ag/As (A) and As/Fe (B), Au/As (C), Au/Ag (D), Cu/Pb (E) and Zn/Pb (F) ratios for all the ICP analyses showing positive correlations.

In the $^{206}Pb/^{204}Pb$ versus $^{207}Pb/^{204}Pb$ diagram, Pb isotope ratios of galena plot between the mantle and the upper crustal curves, especially on the orogene one of the Zartman and Doe curve (Doe and Zartman, 1979; Zartman and Doe, 1981; Megaw, 1998), consistent with a dominantly upper Crustal reservoir with an important contribution of the mantle lead. These Two analyses show clearly that Pb in the ore fluid was a mixture of upper crustal Pb and mantle Pb. During this period, a carbonate platform is installed and accompanied by an intense volcanic activity with locally substitution of the carbonate facies by volcano-sedimentary rocks. This volcanic activity was dated at 533 ± 4 Ma by the U/Pb ion microprobe method (Pouclet *et al*., 2008). The Pb isotope analyse suggests the mantle contribution to the lead source of galena for the Amensif deposit (Fig. 11). These data suggest that the ore-forming materials were probably leached from the Cambro-Ordovician volcano-sedimentary formations. This fluid reacted with a fluid mixture of Permian magmatic water and meteoric water.

5– Discussion

Various theories of ore genesis have been put forward to explain the formation of the Amensif orebodies. The presence of minor amounts of calc-silicate minerals suggests a skarn deposit model. Another model proposed by Managem's prospectors, advocated a veins type. The presence of calc-silicate minerals, led to suggest that the Amensif deposit is a distal magnesian skarn. In this study, we suggest that the origin of the Amensif polymetallic Cu-Pb-Zn-Ag-Au

orebodies is more compatible with the carbonate replacement deposits model.

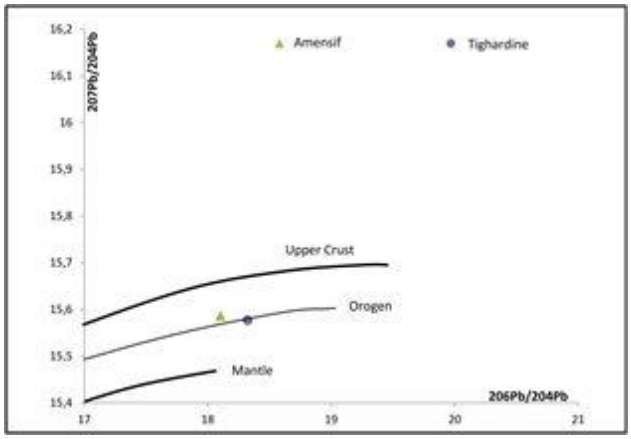

Figure 11: Plots of $^{207}Pb/^{204}Pb$ vs. $^{206}Pb/^{204}Pb$ covariation diagrams for the galena samples from Amensif and Tighardine deposits. Curves of growth trends for Pb isotope ratios are from the plumbotectonic model of Doe and Zartman (1979).

The present study on the Amensif deposit enhances a typical mineralogical and textural evolution of the carbonate-replacement-type deposits Known and described worldwide (Einaudi and Burt; 1982, 1983; Cox, 1986; Morris, 1986; Barton and Bethke, 1987; Eldridge *et al*., 1988; Meinert, 1992; Plumlee *et al*., 1995; Vikre, 1998; Misra, 2000; Meinert *et al*., 2003; Ciobanu and Cook, 2004; Kamona and Freidrich, 2007; Jebrak and Marcoux, 2008). The geological features of the Amensif deposit are comparable to those of many carbonate replacement deposit (Cox, 1986; Morris, 1986; Vikre, 1998; Monteiro *et al*., 2006; Voudouris *et al*., 2008). The principal similarities are tectonic setting, type of host rock, wall-rock alteration, style and mineral composition.

The Amensif Cu, Pb, Zn carbonate hosted rocks is located in the intersection of the Erdouz and Al Medinet fault zones. This geotectonically situation controls the deposition of the main mineralizations and facilitates the circulation of ore-fluids within the fractures and veins. The limestones and dolomites are commonly interstratified with or overlain by volcanic rocks and intruded by porphyritic dikes.

Most of carbonate replacement deposits are characterized by elevated abundances of copper, zinc, lead, iron, arsenic, silver and gold. At Amensif deposit, the metal concentrations are ranging from 0.26 to 4.2 wt. % Cu and 0.77% to 16.07 wt% Zn, 0.49 to 11.25 wt % Pb and 0.47 to 3.24wt % As and 100 to 443 ppm Ag and 0.47 to 4.34 ppm Au. The lead isotope analyse of the galena from the Amensif deposit suggest an important contribution of Cambro-Ordovician mantle rocks.

The contrasts between the coarse-crystalline dolomite and the altered dolomitic limestones of the Lower Cambrian formation indicate that this carbonate formation is affected by an intense replacement and hydrothermal alteration processes taken place close to or within the mineralized zones.

(i) On the basis of upon mineralogical and textural data, the paragenetic sequence is divided into two distinct stages. The first is an arseno-ferriferous stage which marked by cogenetic crystallization of a fin to coarse grained of pyrite and arsenopyrite. It is ended by crystallization of early sphalerite and minor galena. An intensive hydraulic brecciation marked the end of this stage. The second polymetallic stage is dominated by sphalerite with chalcopyrite disease and was also characterized by crystallization of major minerals. Important replacement phenomena were observed between mineral assemblages. A polymetallic assemblage is found by chalcopyrite, sphalerite, galena, pyrite, arsenopyrite, tetrahedrite-tennantite, associated with quartz. The growth habits, textures and association of minerals are also broadly similar

Table 1) Ore samples ICP data.

Samples	Fe (%)	Cu (%)	Pb (%)	Zn (%)	As (ppm)	Ag (ppm)	Au (ppm)
AMC1	8.83	1.38	1.55	1.55	1.43	87	0.62
AMC2	8.71	0.4	0.31	0.89	1.94	39	0.65
AMC3	3.65	0.027	0.13	0.77	0.021	5	0.93
AMC4	2.44	0.086	0.0326	0.21	0.012	4	0.17
AMC5	4.69	0.14	0.47	3.92	0.15	88	0.1
AMC6	2.58	0.0979	0.0819	5.15	0.003	19	0.05
AMC7	7.7	4.2	0.0675	0.15	1.619	236	2
AMC8	4.12	1.47	0.0265	0.0459	1.062	59	0.91
AMC9	4.65	0.081	0.14	4.83	0.003	12	0.05
AMC10	2.58	0.0241	0.0906	0.17	0.023	3	1
AMC11	1.39	0.15	10.07	0.13	0.030	48	0.06
AMC12	9.56	0.84	1.58	6.66	0.010	55	0.09
AMC13	4.51	0.0268	0.25	1.69	0.710	14	2.05
AMC14	29.17	0.15	0.69	2	2.960	53	0.35
AMC15	4.63	2.01	0.11	0.29	1.070	90	0.74
AMC16	2.41	1.49	0.0732	0.1	0.072	81	0.07
AMC17	2.52	0.75	0.0792	0.96	0.014	48	0.05
AMC18	3.69	0.0856	1.92	4.18	0.010	17	-
AMC19	3.8	0.28	2.25	4.88	0.010	45	0.05
AMC20	3.24	0.16	0.02	1.55	0.018	9	0.05
AMC21	2.34	0.26	0.0383	1.98	0.087	24	0.05
AMC22	10.88	1.18	0.0913	0.3	0.477	55	1.03
AMC23	2.58	0.0056	0.0184	5.02	0.047	4	0.05
AMC24	23.16	0.14	0.83	6.61	0.070	56	0.07
AMC25	14.69	0.22	1.18	2.21	0.150	20	0.05
AMC26	20.3	0.52	0.82	16.07	3.240	74	0.07
AMC27	15.72	0.32	0.84	10.84	0.710	114	0.05
AMC28	26.1	0.26	0.49	3.25	3.160	66	0.11
AMC29	2.74	0.0313	0.0219	6.59	0.032	5	0.09
AMC30	16.53	0.42	0.26	11.86	0.560	45	4.34
AMS 11	0.8414	1.66	3.81	0.9	0.860	443	2.32
AMS 16	17.94	2.36	2.43	5.75	1.950	189	1.27
AMS 12	7.68	0.78	11.25	13.91	0.200	251	0.47

to those described worldwide in other comparable deposit (Cox, 1986; Morris, 1986; Vikre, 1998). The remarkable characteristic of this deposit is an extensive replacement textures. These textures have played an important role in the interpretation of the massive sulphide ores. According to Barton and Bethke (1987), the blebs of chalcopyrite observed in sphalerite of this deposit are classified as "chalcopyrite disease". Hydrothermal experiments have clearly shown that the texture could result from either replacement (Eldridge *et al*., 1983, 1988; Ciobanu and Cook, 2004). The origin of this phenomenon of chalcopyrite disease is referred to the selective replacement of the FeS component of the sphalerite by a cooper-bearing solution at higher fs2 (Eldridge *et al*., 1983, 1988; Barton, 1991; Bente and Doering, 1995; Nagase and Kojima, 1997).

(ii) Broad hydrothermal alteration halos of carbonate wall-rocks accompanied the ore deposition. Three major hydrothermal alterations can be observed. Pyrite + quartz + calcite + dolomite minerals characterizing the first alteration. The presence of saddle dolomite (Fig. 5C) indicates a replacement product in some dolomitized limestones (Searl, 1989). Radkhe and Mathis (1980) suggest that it forms at temperatures between 60 and 150°C The second hydrothermal alteration is locally observed (20 m^2) in close contact between carbonate bars and rhyolitic dikes. This skarnification is responsible for the formation of minor anhydrous minerals such as andradite and vesuvianite. These anhydrous minerals are

entirely or partially replaced by latter hydrated (epidote and chlorite) minerals formed during the third hydrothermal alteration. Calagari and Hosseinzadeh (2006), suggest that andradite was stable at temperatures > 430°C within high sulphidation fluid. Finally, the propylitic alteration represents the hydrothermal alteration mostly widespread in the area. Chlorite + epidote + tremolite + sericite +calcite + minor quartz are the most hydrous mineral assemblages characterizing this alteration. These minerals assemblages result from the inflow of cooler fluids that invade the hydrothermal system (Einaudi and Burt, 1982; Cox, 1986; Morris, 1986; Meinert, 1992). The development of this lower-temperature minerals (Calagari and Hosseinzadeh, 2006) suggest that the late metasomatizing fluids were probably at higher oxidation state and had more hydrolyzing nature. The presence of chlorite, tremolite, epidote in metamorphic limestones indicates the interaction between hydrothermal fluid and host rocks and it represents the main indicator for the carbonate replacement deposit type. The same mineral association has been described in the Francisco I. Madero (FIM) Zn-Cu-Pb-(Ag) by Canet *et al*. (2009). According to these authors, the FIM deposit is a distal, dike-related, Zn Skarn akin to the Carbonate Replacement Deposits.

(iii) At the Amensif, the formation of andradites and chalcopyrite disease suppose a high temperature conditions. Barton and Bethke (1987) suggest that chalcopyrite disease could be formed in the 200-400°C range.

(iv) The comparison with others skarn deposits in the world (Permingeat, 1957, Canet *et al*., 2009; 2011; Calagari and Hosseinzadeh, 2006; Oyman, 2010; El khalile *et al*., 2014) indicate that the presence of calc-silicate minerals at the area Amensif is very limited (about 20 m^2). Although no skarn and/or granite are exposed on the surface, minor amounts of skarn are found near than rhyolitic dike. The skarn deposit model appears non applicable to the Amensif pollymetallic deposit. This latter presents very close similarities with "High Temperature Polymetallic Carbonate Replacement Deposit".

6– Conclusion

The Amensif Cu-Pb-Zn-Ag-Au deposit is comparable to "carbonate replacement deposit" in terms of geological setting, tectonic features, ore-host rock, wall-rock alteration and mineral composition. The deposit is hosted within the Lower Cambrian recrystallized carbonates in close space proximity with the copper-molybdenum deposit of the Azegour mine. The tectonic setting with the NE-SW to ENE-WSW and NW-SW faults cross-cutting the area is responsible for the intense fracturation observed. However, the hydrothermal mineral assemblages of Amensif are a result of the hydrothermal fluids that flowing along fractures, stratigraphic contacts and zone of brecciation. Locally, at the immediate contact with the rhyolitic dikes a pervasive silicification was produced and accompanied by crystallization of anhydrous calc-silicates (andradite and vesuvianite). As discussed above the formation of Amensif ore deposit could be divided into three stages stared with pre-ore stage that is characterized by intense hydrothermal alteration. The ore stage (I) is marqued by synchronous deposition of pyrite and arsenopyrite with minor amounts of sphalerite and galena. The ore stage (II) is economically important and is marqued by crystallization of chalcopyrite, sphalerite, galena, arsenopyrite, pyrite and tetraedrite-tennantite. This mineral association was accompanied with invisible gold and silver. The latest stage is characterized by predominance of replacement textures between sulphides. The lead isotopic data show that the ore forming materials are derived from a mixture of upper crustal material and the mantle material. According to lead isotopes data of Amensif and Tighardine deposits, the Pb-Zn-Cu metals were

probably originated from the Lower Paleozoic volcano-sedimentary rocks.

Still being just a hypothesis, this new typology introduced in the western High Atlas area needs more geochemical analysis, fluid inclusion and detailed isotopic study of the host rocks, alteration and mineral assemblages to be finally confirmed.

Acknowledgments:

The authors would like to thank Dr. C. Canet and Dr. S.R. Ghavami Riabi for their appreciate comments which help us to improve manuscript. The present work was financially supported by the Guemassa Mining Company. We would like to thank very much Dr. Eric Marcoux of the Orleans University (France) for the Pb isotope analyse. Special thanks are due to the two anonymous reviewers for their excellent contributions that helped us revise and improve this manuscript.

References:

Ait Ayad, N. 1987. Etude des relations entre déformation et intrusion granitique (l'exemple du granite hercynien d'Azegour. Thesis Cadi Ayyad University, Morocco (in French).

Alansari, A., Bajddi, A., Zouhair, M. 2009. Mise en évidence d'une évolution verticale dans la minéralogie et la typologie des minéralisations à Cu-Zn-Pb-Ag-Ba de Tighardine: Apport à l'exploration minière dans le Haut Atlas Occidental (Maroc). Notes et Mémoires du Service Géologique du Maroc: 530, 31–44 (in French).

Amenzou, M., Badra, L. 1996. Les granites d'Azegour et de Brikiine (Maroc) implications génétique d'après la typologie des Zircons. Comptes rendus de l'Académie des Sciences, Paris : 323, IIa, 213-220 (in French with English Summary).

Badra, L. 1993. Les minéralisations polymétalliques (Pb-Zn-Cu, Ba) du Haut-Atlas Occidental marocain et de ses confins dans leurs cadre géodynamique. Thesis Orléans University, France (in French).

Barton, P. B., Bethke, P. M. 1987. Chalcopyrite disease in sphalerite: pathology and epidemiology. American Mineralogist: 72, 451–467.

Barton, P. B. 1991. Ore textures: problems and opportunities. Mineralogical Magazine: 55, 303–315.

Bente, K., Doering, T. 1995. Experimental studies on the solid state diffusion of Cu + In in ZnS and on "Disease", DIS (Diffusion Induced Segregations), in sphalerite and their geological applications. Mineralogy and Petrology: 53, 285–305.

Bouabdellah, M. 1988. Etude pétrographique et métallogénique du district polymétallique à Pb-Zn-Cu-Ba-Fe et Sn d'Assif El Mal-Bouzouga (Haut-Atlas de Marrakech, Maroc). Thesis Cadi Ayyad University, Morocco (in French).

Bouabdellah, M., Leach, D. L., Johnson, C. 2003. Geochemical characteristics of the Assif El Mal Zn-Pb (Cu, Ag) vein system: High Atlas Mountains, Morocco. In: Eliopoulos *et al*. (eds) Mineral exploration and sustainable development. 7th Biennial SGA-SEG Meeting, Athens, Greece, 949–952.

Bouabdellah, M., Beaudoin, G., Leach, D. L., Grandia, F., Cardellach, E. 2009. Genesis of the Assif El Mal Zn-Pb (Cu, Ag) vein deposit. An extension-related Mesozoic vein system in the High Atlas of Morocco: Structural, mineralogical and geochemical evidence. Mineralium Deposita: 44, 689–704.

Calagari, A. A., Hosseinzadeh, G. 2006. The mineralogy of copper-bearing skarn to the east of the Sungun-Chay River, East-Azarbaidjan, Iran. Journal of Asian Earth Sciences: 28, 423–438.

Canet, C., Camprubi, A., Gonzalez-Partida, E., Linares, C., Alfonso, P., Pineiro-Fernandez, F., Prol-Ledesma, R. M. 2009. Mineral assemblages of the Francisco I- Madero Zn-Cu-Pb-(Ag) deposit, Zacatecas, Mexico: Implications for ore deposit genesis. Ore Geology Reviews: 35, 423–435.

Canet, C., González-Partida, E., Camprubí, A., Castro-Mora, J., Romero, F. M., Prol-Ledesma, R. M., Linares, C., Romero-Guadarrama, J. A., Sánchez-Vargas, L. I. 2011. The Zn-Pb-Ag skarns of Zacatepec, Northeastern Oaxaca, Mexico: A study of

Mineral assemblages and ore-forming fluids. Ore Geology Reviews: 39, 277–290.

Ciobanu, C. L., Cook, N. J., 2004.Skarn textures and a case study: the Ocna de Fier-Dognecea orefield, Banat, Romania. Ore Geology Reviews: 24, 315–370.

Cornée, J. J., Destombes, J., Willefer, S. 1987a. Stratigraphie du Paléozoïque de l'extrémité nord-ouest du Haut Atlas occidental (Maroc hercynien); interprétation du cadre sédimentaire du Maroc occidental. Bulletin de la Société Géologique de France: s. III, 8, 327–335 (in French with English Summary).

Cornée, J. J., Ferrandini, J., Muller, J., Simon, B., 1987b. Le Haut Atlas occidental paléozoïque: un graben cambrien moyen entre deux décrochements dextres N60° E hercyniens (Maroc). Comptes Rendus de l'Académie des Sciences, Paris: 305, 499–503 (in French with English Summary).

Cox, D. P., 1986. Descriptive model of polymetallic veins, in cox D.P. and Singer D.A., eds., Mineral deposit models: U.S. Geol. Survey Bull., 1693.

Dias, R., Hadani, M., Machado, L. I., Adnane, N., Hendaq, Y., Madih, K., Matos, C. 2011. Variscan structural evolution of the western High Atlas and the Haouz plain (Morocco). Journal of African Earth Sciences: 39, 311–318.

Doe, B. R., Zartman, R. E. 1979. Plumbotectonics, the Phanerozoic, in: H.L. Barnes (Ed.), Geochemistry of hydrothermal ore deposits, John Wiley and Sons, New York, 22–70.

Einaudi, M. T., Burt, D. M. 1982. Introduction terminology, classification and composition of skarn deposits. Economic Geology: 77, 745–754.

Eldridge, C. S., Barton, Jr., P. B., Ohmoto, H. 1983. Mineral textures and their bearing on the formation of the Kuroko orebodies. Economic Geology Monographs: 5, 241–281.

Eldridge, C. S., Bourcier, W. L., Ohmoto, H., Barnes, H. L. 1988. Hydrothermal inoculation and incubation of the chalcopyrite disease in sphalerite. Economic Geology: 83, 978–89.

El Amrani, E. I. 1984. Contribution à l'étude pétrologique, minéralogique, métallogénique et pétrologie structurale des formations de la région d'Azegour Haut-Atlas occidental. Thesis Cadi Ayyad University, Morocco (in French).

El Archi, A. 1989. Evolution tectono-sédimentaire et métamorphique d'un ségment paléozoïque du Haut-Atlas occidental (Région Bouzouga et Maghoussa). Thesis Cadi Ayyad University, Morocco (in French).

El Archi, A., El houicha, M., Jouhari, A., Bouabdelli, M. 2004. Is the Cambrian basin of the western High Atlas (Morocco) related either to a subduction zone or a major shear zone? Journal of African Earth Sciences: 39, 311–318.

Ilmen, S. 2011. Contribution à l'étude géologique du Gîte à Cu, Zn, Pb et Ag±Au D'Amensif (Région d'Azegour-Haut Atlas occidental). Master's thesis Cadi Ayyad University, Morocco (in French).

Ivanova, T. I., Shtukenberg, A. G., Punin, Yu. O., Frank-Kamenetskaya, O. V., Sokolov, P. B. 1998. On the complex zonality in grandite garnets and implications. Mineralogical Magazine: 62, 857–868.

Jebrak, M., Marcoux, E. 2008. Géologie des ressources minerals. Ressources naturelles et Faune (ed) Québec, 667pp.

Kamona, A. F., Friedrich, G. H. 2007. Geology, mineralogy and stable isotope geochemistry of the Kabwe carbonate-hosted Pb–Zn deposit, Central Zambia. Ore Geology Reviews: 30, 217–243.

Kovalev, K. R., Kalinin, Yu. A., Naumov, E. A., Kolesnikova, M. K., Korolyuk, V. N. 2011. Gold-bearing arsenopyrite in eastern Kazakhstan gold-sulfide deposits. Russian Geology and Geophysics: 52, 178–192.

Labriki, M. 1996. Carte géologique du Maroc, feuille d'Amezmiz au 1/100 000. Notes et Mémoires du Service Géologique du Maroc : 372 (in French).

Mabkhout, F., Bonin, B., Ait Ayyad, N., Sina, C., Lagarde, J. L. 1988. Les massifs granitiques alcalins du Permien marocain. Comptes Rendus de l'Académie des Sciences, Paris: 507, 163–168, (in French with English Summary).

Megaw, P. K. M. 1998. Carbonate-hosted Pb-Zn-Ag-Cu-Au replacement deposits: an exploration perspective. In: Lentz, D, R. (ED.), Mineralized intrusion skarn systems.

Mineralogical Association of Canada, Short course: 26, 337–413.

Meinert, L. D. 1992. Skarns and skarn deposits. Journal of the Geological Association of Canada: 19, 145–162.

Meinert, L. D., Hedenquist, J. W., Satoh, H., Matsuhisa, Y. 2003. Formation of anhydrous and hydrous skarn in Cu–Au ore deposits by magmatic fluids. Economic Geology: 98, 147–156.

Misra, K. C. 2000. Understanding mineral deposits. Kluwer Academic Dordrecht. 845 pp.

Monteiro, L. V. S., Bettencourt, J. S., Juliani, C., Oliveira, T. F. O. 2006. Geology, petrography, and mineral chemistry of the Vazante non-sulfide and Ambrosia and Fagundes sulfide-rich carbonate-hosted Zn–(Pb) deposits, Minas Gerais, Brazil. Ore Geology Reviews: 28, 201–234.

Morris, H. T. 1986, Descriptive model of polymetallic replacement deposits, in Cox, D.P., and Singer, D.A., eds., Mineral deposit models: U.S. Geological Survey Bulletin 1693, p. 99–100.

Mrini, Z., Rafi, A., Duthou, J. L., Vidal, Ph. 1992. Chronologie Rb-Sr des granitoïdes hercyniens du Maroc. Conséquences. Bulletin de la Société Géologique de France : 163, 281–291 (in French with English Summary).

Nagase, T., Kojima, S. 1997. An SEM examination of the chalcopyrite disease texture and its genetic implications. Mineralogical Magazine: 61, 89–97.

Neltner, L. 1938. Etudes géologiques dans le sud marocain (Haut Atlas et Anti Atlas). Notes et Mémoires du Service Géologique du Maroc: 42, 298 pp. (in French).

Ouanaimi, H., Petit, J. P. 1992. La limite sud de la chaîne hercynienne dans le Haut Atlas marocain: reconstitution d'un saillant non déformé. Bulletin de la Société Géologique de France: 163, 63–72 (in French with English Summary).

Ouazzani, H., Pouclet, A., Badra, L., Prost, A. E. 2001. Le volcanisme d'arc du massif ancien de l'ouest du Haut Atlas occidental (Maroc), un témoin de la convergence de la branche occidentale de l'océan panafricain. Bulletin de la Société Géologique de France: 172, 587–602 (in French with English Summary).

Oyman, T. 2010. Geochemistry, mineralogy and genesis of the Ayazmant Fe–Cu skarn deposit in Ayvalik, (Balikesir), Turkey. Ore Geology Reviews: 37, 175–201.

Permingeat, F. 1957. Le gisement de Molybdènes, Tungstène et Cuivre d'Azegour (Haut-Atlas). Etude pétrographique et métallogénique. Notes et Mémoires du Service Géologique du Maroc : 141 (in French).

Plumlee, G. S., Montour, M, Taylor, C. D., Wallace, A. R., Klein, D. P. 1995. Polymetallic vein and replacement deposits. In du Bray, E. A., ed., 1995, Preliminary compilation of descriptive geoenvironmental mineral deposit models. U.S. Geological Survey Open-File Report 95–831, 121–129.

Pouclet, A., Ouazzani, H., Fekkak, A. 2008. The Cambrian volcano-sedimentary formations of the westernmost High Atlas Morocco): their place in the geodynamic evolution of the West Africain Paleo-Gondwana northern margin. Geological Society of London: 97, 303–327.

Prost, A., Badra, L., El Hasnaoui, H. 1989. Superposition de trois déformations ductiles hercyniennes dans le Haut Atlas (région d'Azegour-Erdouz, Maroc). Comptes rendus de l'Académie des Sciences de Pari : 309, II, 627–632 (in French with English Summary).

Radke, B. M. and Mathis, R. L. 1980. On the formation and occurrence of saddle dolomite. Journal of Sedimentary Petrology: 50, 1149–68.

Ramdohr, P. 1969. The ore minerals and their intergrowths. Pergamon Press. Oxford (2 ed), 1174 pp.

Searl A. 1989. Saddle dolomite: a new view of its nature and origin. Mineralogical Magazine: 53, 547–555.

Stacey J. S., Kramers J. D. 1975. Approximation of terrestrial lead isotope evolution by a two-stage model. Earth and Planetary Science Letters: 26, 207–221.

Vikre, P. G. 1998. Intrusion-related, Polymetallic Carbonate Replacement Deposits in the Eureka District, Eureka County, Nevada. Nevada Bureau of Mines and Geology: 110, 52 pp.

Volkov, A. V., Genkin, A. D., Goncharov, V. I. 2006. Gold species in ores of the Natalkinskoe and Maiskoe deposits (northeastern Russia). Tikhookeanskaya Geologiya: 25, 18–29.

Voudouris, P., Melfos, V., Spry, P. G., Bonsall, T. A., Tarkian, M., Solomos, Ch. 2008. Carbonate-replacement Pb – Zn – Ag ± Au mineralization in the Kamariza area, Lavrion, Greece: Mineralogy and thermochemical conditions of formation. Mineralogy and Petrology: 94, 85–106.

Zartman, R. E., Doe, B. R. 1981. Plumbo-Tectonics, the model. Tectonophysics: 75, 135–162.

Received: 07 February 2014 / Accepted: 01 May 2014 / Published online: 10 May 2014